Your thesaurus codes are: 02.08.1, 03.13.4, 02.18.8, 02.01.2

# General Relativistic Hydrodynamics with Special Relativistic Riemann Solvers

José A. Pons<sup>1</sup>, José A. Font<sup>2</sup>, José M<sup><u>a</u></sup>. Ibáñez<sup>1</sup>,

José M<sup><u>a</u></sup>. Martí<sup>1</sup>, and Juan A. Miralles<sup>1</sup>

<sup>1</sup> Departament d'Astronomia i Astrofísica, Universitat de València, 46100 Burjassot (València), Spain

<sup>2</sup> Max-Planck-Institut f
ür Gravitationsphysik, Albert-Einstein-Institut Schlaatzweg 1, 14473 Potsdam, Germany

Received date; Accepted date

Abstract. We present a general and practical procedure to solve the general relativistic hydrodynamic equations by using any of the special relativistic Riemann solvers recently developed for describing the evolution of special relativistic flows. Our proposal relies on a local change of coordinates in terms of which the spacetime metric is locally Minkowskian and permits accurate numerical calculations of general relativistic hydrodynamics problems using the numerical tools developed for the special relativistic case with negligible computational cost. The feasibility of the method has been confirmed by a number of numerical experiments.

Key words: Hydrodynamics, Methods:numerical, Relativity, Accretion

#### 1. Introduction

In the near future the first generation of Earth-based laser-interferometer detectors of gravitational waves will be operating (LIGO, VIRGO, GEO600, TAMA). This perspective has stimulated researchers working in numerical relativistic astrophysics to develop robust codes for the simulation of the different astrophysical sources of gravitational radiation, such as, e.g., stellar core collapse, coalescing compact binaries or accretion onto compact objects.

Relativistic hydrodynamical codes experienced a substantial advance at the beginning of the nineties (Martí, Ibáñez, Miralles, 1991) with the implementation of high–resolution shock-capturing methods (HRSC) originally developed in classical fluid dynamics. These methods make use of the hyperbolic and conservative character of the equations and display a number of interesting features and properties, as being stable and conservative, converging to physical solutions and having high accuracy in regions where the solution is smooth. They are all based on the resolution of local Riemann problems at the interfaces of numerical cells –following the seminal idea of Godunov (1959) – ensuring a consistent treatment of discontinuities (shocks). The first relativistic applications of these techniques showed their capabilities in describing accurately complex flows, with high Lorentz factors and strong shocks, superseding traditional methods (Wilson 1979) which failed to describe ultrarelativistic flows (Norman and Winkler 1986). Up to now, the use of HRSC methods in relativity has been mainly restricted to the field of special relativistic hydrodynamics (SRH) in the simulation of collisions of heavy ions and, remarkably, extragalactic jets (Martí, Müller and Ibáñez, 1994). We refer the interested reader to the introductory section in Banyuls *et al.* (1997) for a recent review of the current status of HRSC techniques in numerical relativistic hydrodynamics.

In recent years, the great success obtained in the first relativistic applications has drawn the attention of specialists who started to develop specific Riemann solvers for SRH. Nowadays, most of the reliable HRSC methods developed during the last twenty years in classical hydrodynamics have their special-relativistic extension (see, e.g., Ibáñez *et al.*, 1997, for an updated list). In the case of general relativistic hydrodynamics (GRH), the development of numerical codes based on the resolution of local Riemann problems is still in its infancy. Only a small number of papers have considered the extension of HRSC methods from SRH to GRH (see below). In addition, recently, several formulations of Einstein Equations as a first-order hyperbolic system of balance laws have been derived (Friedrich 1985; Bona *et al.* 1995; Abrahams *et al.* 1995; Fritelli & Reula 1996). This opens a new strategy, in the field of Numerical Relativity, permitting the use of HRSC schemes, specifically designed for such hyperbolic systems, to solve the coupled system of spacetime plus hydrodynamics (Bona *et al.* 1993).

The basic idea behind this work is to obtain a general procedure that allows us to take advantage of the increasing number of special relativistic Riemann solvers (SRRS) developed recently, in order to generate numerical solutions describing the evolution of relativistic flows in strong gravitational fields (background or dynamical). All the previous works done to extend HRSC methods to GRH have used linearized Riemann solvers (Martí, Ibáñez, Miralles 1991; Eulderink and Mellema 1994; Romero *et al.* 1996; Banyuls *et al.* 1997). In this paper we describe a procedure to use any type of SRRS in general relativistic hydrodynamics, including the exact Riemann solver for 1D problems. This procedure relies on a local change of coordinates at each numerical interface, in terms of which the spacetime metric is locally flat, analogously to the approach followed in classical fluid dynamics, when using the solution of Riemann problems in general curvilinear coordinates. The numerical implementation is simple, computationally inexpensive, and provides a useful tool for the researchers currently working in SRH to enter the field of GRH.

The structure of this paper is the following: In §2 we summarize the GRH equations in the  $\{3 + 1\}$  formalism and the basic ideas of HRSC methods. In §3 the formulation of Riemann problems in locally flat spacetimes and the method to obtain the numerical fluxes for the GRH equations from those obtained in SRH is explained. In §4 we briefly describe the set of numerical tests and applications performed to demonstrate the feasibility of the approach. Finally, in §5 we summarize our results and foresee other applications of our proposal.

#### 2. GRH equations in the 3+1 formalism and HRSC methods.

Let  $\mathcal{M}$  be a general spacetime, described by the four dimensional metric tensor **g**. The line element has the form

$$ds^2 = -(\alpha^2 - \beta_i \beta^i) dt^2 + 2\beta_i dx^i dt + \gamma_{ij} dx^i dx^j$$
(1)

Throughout the paper Greek (Latin) subscripts run from 0 to 3 (1 to 3) and geometrized units are used (G = c = 1). Let  $\{\partial_t, \partial_i\}$  be the coordinate basis and **n** the unit timelike vector field normal to the spacelike hypersurfaces  $\Sigma_t$  (t = const.)

$$\partial_t = \alpha \mathbf{n} + \beta^i \partial_i \tag{2}$$

We denote by  $\mathbf{J}$  and  $\mathbf{T}$  the density current and the energy–momentum tensor for a perfect fluid, respectively,

$$\mathbf{J} = \rho \mathbf{u} \tag{3}$$

$$\mathbf{T} = \rho h \mathbf{u} \otimes \mathbf{u} + p \mathbf{g} \tag{4}$$

with **u** the four-velocity of the fluid,  $\rho$  the rest-mass density, p the pressure and h the specific enthalpy ( $h = 1 + \epsilon + p/\rho$ , where  $\epsilon$  is the specific internal energy).

The equations describing the evolution of a relativistic fluid are the *local conservation* laws of baryon number and energy-momentum and can be written, for observers which are at rest in the slice  $\Sigma_t$  (Eulerian observers), in terms of the divergence of the 5 vector fields {J,  $\mathbf{T} \cdot \mathbf{n}, \mathbf{T} \cdot \partial_1, \mathbf{T} \cdot \partial_2, \mathbf{T} \cdot \partial_3$ } as,

$$\nabla \cdot \mathbf{A} = s,\tag{5}$$

where **A** denotes any of the above 5 vector fields and s is the corresponding source term. Explicit expressions of these vectors in terms of the *primitive variables* { $\rho, \epsilon, v_i$ } (with  $v_i$  the components of the velocity measured by an Eulerian observer), as well as expressions for the source terms, are given in Banyuls et al. (1997).

Let us consider the integral form of the above equations on a four-dimensional volume  $\Omega \subset \mathcal{M}$  with three-dimensional boundary  $\partial \Omega$ , and apply Gauss theorem to obtain the corresponding balance equation

$$\int_{\partial\Omega} \mathbf{A} \cdot d^3 \mathbf{\Sigma} = \int_{\Omega} s d\Omega.$$
(6)

For numerical applications, we choose the volume  $\Omega$  as the one bounded by the coordinate hypersurfaces  $\{\Sigma_{x^{\alpha}}, \Sigma_{x^{\alpha}+\Delta x^{\alpha}}\}$ . Hence, the time variation of the mean value of  $A^{0}$ ,

$$\overline{A}^{0} = \frac{1}{\Delta \mathcal{V}} \int_{x^{1}}^{x^{1} + \Delta x^{1}} \int_{x^{2}}^{x^{2} + \Delta x^{2}} \int_{x^{3}}^{x^{3} + \Delta x^{3}} \sqrt{-g} A^{0} dx^{1} dx^{2} dx^{3},$$
(7)

within the spatial volume

$$\Delta \mathcal{V} = \int_{x^1}^{x^1 + \Delta x^1} \int_{x^2}^{x^2 + \Delta x^2} \int_{x^3}^{x^3 + \Delta x^3} \sqrt{-g} dx^1 dx^2 dx^3, \tag{8}$$

can be obtained from

$$(\overline{A}^{0}\Delta\mathcal{V})_{t+\Delta t} = (\overline{A}^{0}\Delta\mathcal{V})_{t} + \int_{\Omega} sd\Omega - \left(\int_{\Sigma_{x^{1}}} \mathbf{A} \cdot d^{3}\boldsymbol{\Sigma} + \int_{\Sigma_{x^{1}+\Delta x^{1}}} \mathbf{A} \cdot d^{3}\boldsymbol{\Sigma} + \int_{\Sigma_{x^{2}}} \mathbf{A} \cdot d^{3}\boldsymbol{\Sigma} + \int_{\Sigma_{x^{2}+\Delta x^{2}}} \mathbf{A} \cdot d^{3}\boldsymbol{\Sigma} + \int_{\Sigma_{x^{3}}} \mathbf{A} \cdot d^{3}\boldsymbol{\Sigma} + \int_{\Sigma_{x^{3}+\Delta x^{3}}} \mathbf{A} \cdot d^{3}\boldsymbol{\Sigma} \right).$$

$$(9)$$

In order to update the solution in time, the volume and surface integrals on the right hand side of Eq (9) have to be evaluated (see §3). HRSC schemes rely on the calculation of the **A** vector fields by solving local Riemann problems combined with monotonized cell reconstruction techniques.

## 3. Formulation of Riemann Problems in locally Minkowskian coordinates.

According to the equivalence principle, physical laws in a *local inertial frame* of a curved spacetime have the same form as in special relativity. Locally flat (or geodesic) systems of coordinates, in which the metric is brought into the Minkowskian form up to second order terms, are the realization of these local inertial frames. However, whereas the coordinate transformation leading to locally flat coordinates involves second order terms, locally Minkowskian coordinates are obtained by a linear transformation. This fact is of crucial importance when exploiting the selfsimilar character of the solution of the Riemann problems set up across the coordinate surfaces.

Hence, we propose to perform, at each numerical interface, a coordinate transformation to locally Minkowskian coordinates assuming that the solution of the Riemann problem is the one in special relativity and planar symmetry. This last assumption is equivalent to the approach followed in classical fluid dynamics, when using the solution of Riemann problems in slab symmetry for problems in cylindrical or spherical coordinates, which breaks down near the singular points (*e.g.* the polar axis in cylindrical coordinates). Analogously to classical fluid dynamics, the accuracy will depend on the magnitude of the Christoffel symbols, which might be large whenever huge gradients or large temporal variations of the gravitational field are present. Finer grids and improved time advancing methods will be required in those regions.

In the rest of this section we will focus on the evaluation of the first flux integral in Eq. (9).

$$\int_{\Sigma_{x^1}} \mathbf{A} \cdot d^3 \mathbf{\Sigma} = \int_{\Sigma_{x^1}} A^1 \sqrt{-g} \, dx^0 dx^2 dx^3 \tag{10}$$

To begin, we will express the integral on a basis  $\mathbf{e}_{\hat{\alpha}}$  with  $\mathbf{e}_{\hat{0}} \equiv \mathbf{n}$  and  $\mathbf{e}_{\hat{i}}$  forming an orthonormal basis in the plane orthogonal to  $\mathbf{n}$  with  $\mathbf{e}_{\hat{1}}$  normal to the surface  $\Sigma_{x^1}$  and  $\mathbf{e}_{\hat{2}}$  and  $\mathbf{e}_{\hat{3}}$  tangent to that surface. The vectors of this basis verify  $\mathbf{e}_{\hat{\alpha}} \cdot \mathbf{e}_{\hat{\beta}} = \eta_{\hat{\alpha}\hat{\beta}}$  with  $\eta_{\hat{\alpha}\hat{\beta}}$  the Minkowski metric (in the following, caret subscripts will refer to vector components in this basis).

Denoting by  $x_0^{\alpha}$  the coordinates of the center of the interface at time t, we introduce the following locally Minkowskian coordinate system

$$x^{\hat{\alpha}} = M^{\hat{\alpha}}_{\alpha} (x^{\alpha} - x^{\alpha}_0), \tag{11}$$

where the matrix  $M^{\hat{\alpha}}_{\alpha}$  is given by  $\partial_{\alpha} = M^{\hat{\alpha}}_{\alpha} \mathbf{e}_{\hat{\alpha}}$ , calculated at  $x^{\alpha}_{0}$ . In this system of coordinates the flux terms in the equations of GRH are written as in SRH, in Cartesian coordinates, and the flux integral (10) reads

$$\int_{\Sigma_{x^1}} (A^{\hat{1}} - \frac{\beta^1}{\alpha} A^{\hat{0}}) \sqrt{-\hat{g}} \, dx^{\hat{0}} dx^{\hat{2}} dx^{\hat{3}} \tag{12}$$

with  $\sqrt{-\hat{g}} = 1 + \mathcal{O}(x^{\hat{\alpha}})$ , where we have taken into account that, in the coordinates  $x^{\hat{\alpha}}$ ,  $\Sigma_{x^1}$  is described by the equation  $x^{\hat{1}} - \frac{\beta^{\hat{1}}}{\alpha}x^{\hat{0}} = 0$  (with  $\beta^{\hat{i}} = M_i^{\hat{i}}\beta^i$ ), where the metric elements  $\beta^1$  and  $\alpha$  are calculated at  $x_0^{\alpha}$ . Therefore, the effect of a non-zero shift is that the interface where the Riemann problem has to be solved is not at rest but moves with speed  $\beta^{\hat{1}}/\alpha$ .

At this point, all the theoretical work developed in the last years, concerning SRRS, can be exploited. The procedure involves the following steps:

1) We set up the Riemann problem by giving the values at the two sides of  $\Sigma_{x^1}$  of two independent thermodynamical variables (namely, the rest mass density  $\rho$  and the specific internal energy  $\epsilon$ ) and the components of the velocity in the orthonormal spatial basis  $v^{\hat{i}}$ , which are calculated using

$$v^{\hat{i}} = M_i^{\hat{i}} v^i \tag{13}$$

where

$$M_{i}^{\hat{i}} = \begin{pmatrix} \frac{1}{\sqrt{\gamma^{11}}} & \frac{-\gamma^{12}\gamma_{22}+\gamma^{13}\gamma_{23}}{\gamma^{11}\sqrt{\gamma_{22}}} & \frac{-\gamma^{13}\sqrt{\gamma_{22}\gamma_{33}-(\gamma_{23})^{2}}}{\gamma^{11}\sqrt{\gamma_{22}}} \\ 0 & \sqrt{\gamma_{22}} & 0 \\ 0 & \frac{\gamma_{23}}{\sqrt{\gamma_{22}}} & \frac{\sqrt{\gamma_{22}\gamma_{33}-(\gamma_{23})^{2}}}{\sqrt{\gamma_{22}}} \end{pmatrix}$$
(14)

2) The special relativistic Riemman problem is solved for the variables  $\rho$ ,  $\epsilon$  and  $v^{\hat{i}}$ , obtaining the fluxes associated to  $\mathbf{J}, \mathbf{T} \cdot \mathbf{n}, \mathbf{T} \cdot \mathbf{e}_{\hat{j}}$ . Notice that the effect of a non-zero shift has to be considered at this stage. Although most linearized Riemann solvers provide the numerical fluxes for surfaces at rest, it is easy to generalize them to moving surfaces relying on the conservative and hyperbolic character of the system of equations (see, *e. g.*, Harten and Hyman 1983).

3) Once the Riemann problem has been solved, by means of any linearized or exact SRRS, we can take advantage of the selfsimilar character of the solution of the Riemann problem, which makes it constant on the surface  $\Sigma_{x^1}$  simplifying enormously the calculation of the above integral (12):

$$\int_{\Sigma_{x^1}} \mathbf{A} \cdot d^3 \mathbf{\Sigma} = (A^{\hat{1}} - \frac{\beta^{\hat{1}}}{\alpha} A^{\hat{0}})^* \int_{\Sigma_{x^1}} \sqrt{-\hat{g}} \, dx^{\hat{0}} dx^{\hat{2}} dx^{\hat{3}}$$
(15)

where the superscript (\*) stands for the value on  $\Sigma_{x^1}$  obtained from the solution of the Riemann problem. The quantity in parenthesis in Eq. (15) represents the numerical flux across  $\Sigma_{x^1}$ . Notice that the numerical fluxes correspond to the vector fields  $\mathbf{J}, \mathbf{T} \cdot \mathbf{n}, \mathbf{T} \cdot e_{\hat{1}},$  $\mathbf{T} \cdot e_{\hat{2}}, \mathbf{T} \cdot e_{\hat{3}}$ . In order to obtain the momentum fluxes in the original coordinates  $(\mathbf{T} \cdot \partial_i)$ the additional relation

$$\mathbf{T} \cdot \partial_i = M_i^{\hat{j}} (\mathbf{T} \cdot \mathbf{e}_{\hat{j}}) \tag{16}$$

has to be used.

4) Finally, the numerical fluxes are multiplied by the surface integral appearing at the right hand side of (15), that is expressed in terms of the original coordinates as

$$\int_{\Sigma_{x^1}} \sqrt{\gamma^{11}} \sqrt{-g} \, dx^0 dx^2 dx^3 \tag{17}$$

and can be easily evaluated for a given metric.

Let us remind that, in this section, we have focussed on the calculation of the flux terms in Eq. (9), for given left and right states. Obviously, the performance of the numerical code depends on the quality of the provided initial states, as well as the computation of the source terms in Eq. (9), and the algorithm for time advancing. In all the calculations presented in next section, left and right states for Riemann problems have been obtained with a monotonic, piecewise linear reconstruction procedure. The source integrals have been evaluated assuming constant values of  $\rho$ ,  $\epsilon$  and  $v^i$  inside the numerical cells. Finally, advance in time has been done by means of a TVD-preserving, third order Runge-Kutta, that takes into account the influence of the source terms in the intermediate steps. Notice that the treatment of the source terms is essential for the method to work in regions where they dominate. A treatment consistent with the reconstruction procedure and better time advancing schemes may be required in regions very close to coordinate singularities, where the source terms might diverge.

## 4. Tests and applications.

In order to demonstrate the feasibility of our procedure we have considered an exhaustive sample of standard discontinuous initial value problems for which the exact solution is known, as well as some numerical applications involving strong gravitational fields. The set of SRRS used in the computations are the exact one (Martí and Müller 1994) for 1D problems, as well as SR extensions of the linearized solvers described in Harten, Lax and van Leer (1983), Roe (1981), and Donat and Marquina (1996).

To summarize, we have successfully redone all the experiments shown in Banyuls *et al.* (1997), that includes relativistic shock-tube tests for non-diagonal metrics, as well as a number of simulations of relativistic wind accretion onto a Schwarzschild black hole. In Figure 1, we show the results from a simulation of spherical accretion of an ideal gas onto a Schwarzschild black hole. The analytical solution derived by Michel (1972) is represented by the solid line and the diamonds represent the numerical solution obtained using the exact SRRS, after the stationary state has been reached. In Figure 2, we display results from two dimensional simulations of non-spherical accretion onto a moving black hole, corresponding to one of the models recently studied in Font & Ibañez (1998) [model MC2 in their table I]. The figure displays isocontours of the rest mass density in logarithmic scale. The upper-left panel displays the results obtained from the code described in Banyuls *et al.* (1997), the upper-right panel shows the results obtained with the new approach using the same solver (Roe-like). Results obtained with the new approach using HLLE and Marquina's solvers are shown in the lower-left and lower-right panels, respectively.

The main conclusion emerging from the comparison is that our new approach generates remarkably similar results for the four different SRRS, the tiny differences being due to the intrinsic properties of each solver, e.g., Roe's solver is the least diffusive and therefore more oscillatory. The results following the method presented in Banyuls *et al.*  (1997) are indistinguishable from the ones obtained using the special relativistic Roelike solver in this new approach. It can be shown analytically that both algorithms are equivalent.

#### 5. Conclusions and outlook

We have developed a general procedure to use SRRS in multidimensional general relativistic hydrodynamics that allows us to take advantage of the increasing number of SRRS developed recently, overcoming partial approaches derived in previous papers, which were restricted to linearized Riemann solvers. Since the change of coordinates we propose is linear and only involves a few arithmetical operations, the additional computational cost of the approach is completely negligible.

The procedure has a large potentiality and could be applied to other systems of conservation laws, as the equations of general relativistic magneto-hydrodynamics, providing a very useful numerical tool to solve them using the corresponding Riemann solvers developed for the special relativistic case. The feasibility of the approach has been extensively tested and its numerical performance is, at least, as good as other schemes developed in previous papers, having the additional advantage of being very well suited to include future work and improvements that might be done in the field of SR Riemann solvers.

Acknowledgements. This work has been supported by the Spanish DGICYT (grant PB94-0973). J. M<sup><u>a</u></sup>. M. and J.A.F have benefited from European contracts (nrs. ERBFMBICT950379 and ERBFMBICT971902, respectively) . J.A.F. also acknowledges previous financial support from the MPG to work at the AEI in Potsdam. The authors thank M.A. Aloy, S. Brandt, J. Ferrando, P. Papadopoulos, M. Portilla and E. Seidel for useful discussions.

## References

Abrahams, A., Anderson, A., Choquet-Bruhat, Y., and York, J.W., 1995, Phys. Rev. Lett., 75, 3377.

Banyuls, F., Font, J. A., Ibáñez, J. M<sup>a</sup>., Martí, J. M<sup>a</sup>., and Miralles, J.A., 1997, ApJ, 476, 221.

Bona, C., Massó, J., Seidel, E., and Stela, J., 1995, Phys. Rev. Lett., 75, 600.

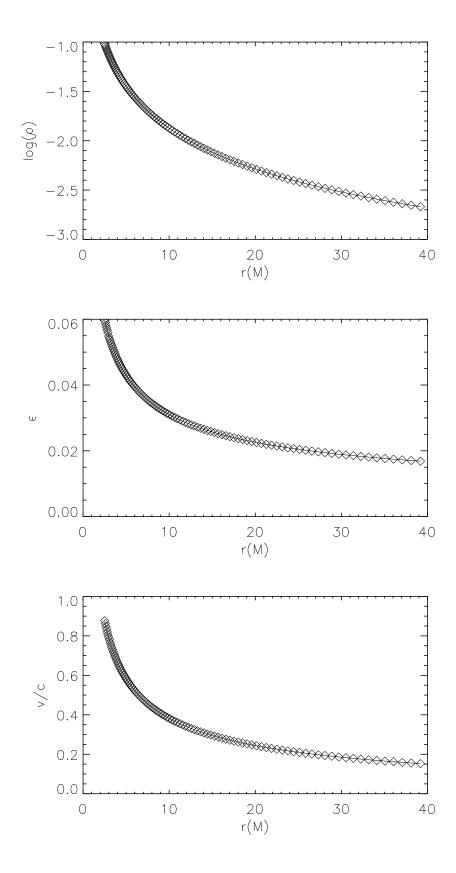
- Bona, C., Ibáñez, J.M<sup>a</sup>., Martí, J.M<sup>a</sup>., and Massó, J., 1993, in *Gravitation and General Relativity: Rotating Bodies and Other Topics*, edited by F. Chinea and L.M. Gonzáles-Romero (Springer Verlag, Berlin).
- Donat, R. and Marquina, A., 1996, J. Comput. Phys., 125, 42.
- Eulderink, F., and Mellema, G., 1994, A&A, 284, 652.
- Font, J.A., Ibáñez, J. M<sup>a</sup>., Marquina, A. and Martí, J.M<sup>a</sup>., 1994, A&A, 282, 304.
- Font, J.A. and Ibáñez, J. M<sup>a</sup>., 1998, ApJ, 494, 297.
- Friedrich, H., 1985, Comm. Math. Phys., 100, 525.
- Fritelli, S., and Reula, O., 1996, Phys. Rev. Lett., 76, 4667.

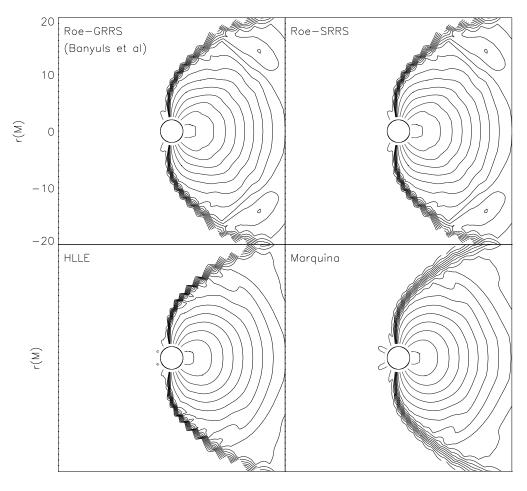
- Godunov, S.K., 1959, Mat. Sb., 47, 271.
- Harten, A. and Hyman, J.M., 1983, J. Comput. Phys., 50, 235.
- Harten, A., Lax, P.D., and van Leer, B., 1983, SIAM Review, 25, 35.
- Ibáñez, J. M<sup><u>a</u></sup>., et al., 1997, in Proceedings from the 18th. Texas Sym. on Relativistic Astrophysics, World Scientific Press.
- Martí, J.M<sup>a</sup>., Ibáñez, J. M<sup>a</sup>., and Miralles, J.A., 1991, Phys. Rev., D43, 3794.
- Martí, J.M<sup><u>a</u></sup>., and Müller, E., 1994, J. Fluid Mech., 258, 317.
- Martí, J.M<sup><u>a</u></sup>., Müller, E., and Ibáñez, J. M<u><sup>a</sup></u>., 1994, A&A, 281, L9.
- Michel, F. C., 1972, Ap&SS, 15, 153.
- Norman, M.L., and Winkler, K-H.A., 1986, Astrophysical Radiation Hydrodynamics, (Reidel).
- Romero, J.V., Ibáñez, J. M<sup>a</sup>., Martí, J.M<sup>a</sup>., and Miralles, J.A., 1996, ApJ, 462, 836.
- Roe, P.L., 1981, J. Comput. Phys., 53, 357.

Wilson, J.R., 1979, in Sources of gravitational radiation, (Cambridge University Press).

Fig.1. Spherical accretion of an ideal gas: profiles of density ( $\rho$ ), internal energy ( $\epsilon$ ) and velocity (v/c) as a function of the radial coordinate, after the steady state has been reached. The critical point ( $r_c$ ), the critical density at the critical point ( $\rho_c$ ) and the adiabatic exponent of the equation of state ( $\gamma$ ) have been taken  $r_c = 200M$ ,  $\rho_c = 7 \times 10^{-4}$  and  $\gamma = 4/3$ . The solid line corresponds to the analytic solution and the diamonds to the numerical one obtained using the exact SRRS.

Fig.2. Non-spherical hydrodynamic accretion onto a Schwarzshild black hole. The initial model is characterized by an asymptotic velocity of 0.5c and Mach number 5. The adiabatic exponent of the fluid is 5/3. The simulation employs a grid of  $120 \times 40$  zones in the radial and polar directions respectively. The radial domain extends from 2.1M to 38M. The polar domain extends from 0 to  $\pi$ . The flow moves from left to right. The different pannels show isocontours of the logarithm of the density normalized to its asymptotic value. Starting from the upper-left pannel and in a clockwise sense we show results for the Roe solver (as used in Banyuls et al (1997)), its SRRS version, Marquina's solver and HLLE. The isocontours span the same interval regardless of the solver used. This range goes from 0 to 1.15. The maximum values are always found at the rear part of the hole where the matter piles up. The different solvers agree on this value up to three significant figures.





r(M)

r(M)